JMEPEG (2017) 26:554–562
DOI: 10.1007/s11665-016-2400-1

1059-9495/$19.00

Twin-Induced Plasticity of an ECAP-Processed TWIP Steel

L. Wang, J.A. Benito, J. Calvo, and J.M. Cabrera

(Submitted March 10, 2016; in revised form October 5, 2016; published online December 21, 2016)

The TWIP steels show high strain hardening rates with high ductility which results in high ultimate tensile strength. This makes their processing by equal channel angular pressing very difficult. Up to now, this has only been achieved at warm temperatures (above 200 °C). In this paper, a FeMnCAl TWIP steel has been processed at room temperature and the resulted microstructure and mechanical properties were investigated. For comparison, the material has also been processed at 300 °C. The TWIP steel processed at room temperature shows a large increase in yield strength (from 590 in the annealed condition to 1295 MPa) and the ultimate tensile strength (1440 MPa) as a consequence of a sharp decrease in grain size and the presence within the grains of a high density of mechanical twins and subgrains. This dense microstructure results also in a loss of strain hardening and a reduction in ductility. The material processed at 300 °C is more able to accommodate deformation and has lower reduction in grain size although there is a significant presence of mechanical twins and subgrains produced by dislocation activity. This material reaches an ultimate tensile strength of 1400 MPa with better ductility than the room temperature material.

Keywords ECAP, EBSD, mechanical properties, twins, TWIP steels

1. Introduction

Nowadays, both from an environmental and from an economic point of view, the demand of lightweight materials in the automotive industry is increasing constantly. According to some statistics, a weight reduction in a car of 10% promotes a fuel consumption reduction between 3 and 7% (Ref 1, 2). Therefore, the optimization and upgrading of steels, which account for 55 to 70% of the total vehicle weight, is extremely important.

Austenitic high-Mn (15-30 wt.%) steels showing twinning-induced plasticity (TWIP) provide great potential in applications for structural components in the automotive industry, owing to their excellent tensile strength-ductility combination. This makes these steels as ideal candidates for energy absorption applications, such as automotive crash safety components and vehicle armor (Ref 3). The exceptional mechanical behavior is triggered by the value of the stacking fault energy (SFE) of these particular steels. It is well known that the active deformation mechanism depends on SFE, which is controlled by the temperature and the composition. At low SFE values, the deformation mechanism is mainly controlled by martensitic transformation [transform-induced plasticity (TRIP) effect]. At increasing SFE, twinning-induced plasticity (TWIP effect) becomes the governing mechanism. Finally, at large SFE values, dislocation glide is the active mechanism (Ref 4, 5). In order to promote a TWIP effect, the SFE values have range between 12-35 mJ/m^2 (Ref 4). The high strength attained by TWIP steels is attributed to a dynamic Hall-Petch effect (Ref 3, 6, 7): deformation progresses by the formation of twins which act as obstacles for dislocation gliding. This process results in a limitation of the dislocation mean free path, leading to a high hardening behavior while large ductility is due to the plasticity promoted by the twinning transformation.

When compared to other advanced high strength steels (AHSS), the wide spread use of TWIP steels is limited, especially in the vehicle industry, because of their relatively low yield strength (Ref 3). In order to solve this problem, some solutions have been proposed and explored in the literature, namely: precipitation hardening (Ref 6, 8-11) and grain refinement by thermo-mechanical processing (Ref 12-14). However, the alternative way to promote grain refinement by severe plastic deformation (SPD) has not been yet explored enough.

It is widely recognized nowadays that SPD is an efficient method to enhance the yield and ultimate strength. Matoso et al. (Ref 15) conducted high-pressure torsion (HPT) procedure on a Fe-Mn-Al-Si TWIP steel and found that the hardness increased sharply. However, the strain hardening was lost because twinning was exhausted during the deformation. Abramova et al. (Ref 16) applied HPT at different temperatures and found different deformation mechanisms. Another method of SPD, equal channel angular pressing (ECAP) is also considered an efficient one. Through this multi-step technique, a large amount of shear strain can be introduced in the processed samples after every pass, with no change in the transversal section of the workpiece, refining the microstructure of the processed material and resulting in improvements in both physical and mechanical properties. Particularly, ECAP can introduce large strains in the deformation process and increase the dislocation density quickly.

L. Wang, School of Materials Science and Engineering, Xian Petroleum University, Xi'an 710065, China and Department of Materials Science and Metallurgical Engineering, ETSEIB, Universitat Politècnica de Catalunya, Av. Diagonal 647, 08028 Barcelona, Spain; **J.A. Benito**, Department of Materials Science and Metallurgical Engineering, ETSEIB, Universitat Politècnica de Catalunya, Av. Diagonal 647, 08028 Barcelona, Spain and Department of Materials Science and Metallurgical Engineering, EUETIB, Universitat Politècnica de Catalunya, Comte d'Urgell 187, 08036 Barcelona, Spain; and **J. Calvo** and **J.M. Cabrera**, Department of Materials Science and Metallurgical Engineering, ETSEIB, Universitat Politècnica de Catalunya, Av. Diagonal 647, 08028 Barcelona, Spain and CTM Technology Center, Plaça de la Ciència 2, 08242 Manresa, Spain. Contact e-mail: richard0723@163.com.

There is scarce information on the application of ECAP for TWIP steels. In fact, it is hard to carry out ECAP on TWIP steel due to their extremely high strength and high ductility. Bagherpour et al. (Ref 17) conducted ECAP at room temperature for TWIP steels in an ECAP die of $\Phi = 120°$ observing a large number of cracks and concluded that flow localization was in the basis of the onset of fracture. The attempts to process TWIP steel in ECAP dies with $\Phi = 90°$ at room temperature have failed due mainly to fractures in the punch, and it has only been possible when the temperature has been increased to 300 °C (Ref 18, 19). By this process, good results have been obtained but high temperature could lead to either dynamic or static recrystallization and therefore grain size refinement is limited. Furthermore, the twin fraction can decrease at high temperature (Ref 20, 21) and some change in the deformation mechanism of TWIP steels could be expected (Ref 22). The introduction of an outer angle ψ in the typical ECAP die with $\Phi = 90°$ has proven to be a good solution to extrude high strength or high ductility materials (Ref 23, 24). On this basis, the use of an ECAP die with an outer angle ψ with high curvature should increase the chances of success in processing the TWIP steel by ECAP at room temperature.

This work has the aim to process a TWIP steel by ECAP at room temperature and to characterize the microstructural evolution and the mechanical properties. The results will be compared with the case of a TWIP steel processed by ECAP at the usual temperature of 300 °C. For this, samples extracted from the extruded bars at both temperatures will be tested by tensile tests. At the same time, the microstructure of both materials will be characterized by electron back-scattered diffraction (EBSD) and transmission electron microscopy (TEM) in order to interpret the influence of microstructural changes in the mechanical properties of the processed materials.

2. Experimental Procedure

The chemical composition of the steel under study is listed in Table 1. Moreover, in this table, the calculated value of SFE according to Ref 25, 26 is also included. In particular, the SFE is calculated based on the formula (Ref 26):

$$\Gamma = 2\rho\Delta G^{\gamma\to\varepsilon} + 2\sigma^{\gamma/\varepsilon} \quad \text{(Eq 1)}$$

where Γ is the SFE of austenite, ρ is the atomic density of the close-packed plane in FCC crystal structure, $\Delta G^{\gamma\to\varepsilon}$ is the difference in the chemical free energy between austenite and epsilon martensite phase, and $\alpha^{\gamma/\varepsilon}$ is the inter-facial energy between austenite and epsilon martensite phase. The value for the present steel is 27.3 mJ/m^2, within the range of values for which twinning is an active deformation mechanism at room temperature.

The material was received as a hot-rolled plate of 15 mm in thickness. ECAP cylindrical samples with 60 mm in length and 8 mm in diameter were machined from the above plate. For homogenization purposes, these bars were annealed for 60 min at 1200 °C in a protective Ar inert atmosphere followed by water quenching, giving as a result a material with an average grain size of 99 μm (twin boundaries were not considered).

Table 1 Chemical composition of the FeMnCAl TWIP steel in weight percent and the calculated stacking fault energy after Ref 25, 26

C	Mn	Si	Al	Fe	SFE
0.5	20.1	1.23	1.72	Bal.	27.3 mJ/m^2

The ECAP was performed in a die made of a tool steel with two channels intersecting at an inner angle of $\Phi = 90°$ and an outer angle of $\psi = 37°$ (see Fig. 1), resulting in a strain of 1 per pass, according to the Iwahashi's relationship (Ref 23). The axis reference system xyz is also illustrated in Fig. 1 with special emphasis on indicating the extrusion direction "x" (ED), the normal direction "y" (ND) and the transversal direction "z" (TD). MoS_2 was used as a lubricant, and the extrusion speed was 0.002 m/s. In the case of room temperature process, it was only possible to extrude the material one pass. In the second pass, there were different problems related with fractures of the punch and breakage of the samples. For comparison, the material was also processed at 300 °C for one pass. For this purpose, the die was placed inside a furnace for warm temperature processing and it was heated to 300 °C, then the sample was introduced in the die and left to warm during 5 min before processing.

The tensile samples were machined from the longitudinal section of the ECAP samples as displayed in Fig. 2(a). The dimensions of the micro-tensile samples used in this work are shown in Fig. 2(b). The tensile tests were carried out in a Microtest DEBEN machine with a cross head speed of 3.3×10^{-3} mm/s (quasi-static loading conditions). The fracture surfaces were analyzed under scanning electron microscope with a Field Emission Gun JEOL JSM-7001F (FE SEM) operated at 20 kV.

The grain size was measured by electron back-scattered diffraction (EBSD) on the transverse plane (xy plane). The samples were cut from the center of the ECAP specimens and mechanically polished using 0.02 μm colloidal silica solution. High resolution orientation maps were acquired through a scanning electron microscope (SEM) with a Field Emission Gun JEOL JSM-7001F (at a voltage of 20 kV) operating with the Oxford Instruments HKL Channel 5 software. Different step sizes were used: 3 μm for the annealed TWIP steel, 0.2 μm for the samples with 1 ECAP pass at 300 °C, 0.08 μm for the samples with 1 ECAP pass at room temperature. The orientation color code used in this paper is given by the standard triangle of inverse pole figure (IPF): grains misoriented with respected to the ⟨100⟩, ⟨110⟩, ⟨111⟩ orientations are red, green and blue, respectively.

Further microstructure examination was performed through transmission electron microscopy (TEM). The specimens were analyzed in a Philips C2100 microscope operating at 200 kV. The samples for TEM observation were mechanically polished to 40 μm in thickness and then thinned by twin-jet electron polishing in an electrolyte solution of 95 vol.% acetic acid glacial and 5% perchloric acid at room temperature.

3. Results

3.1 Microstructure Characterization

3.1.1 EBSD Characterization. Figure 3 shows the microstructure of the annealed and ECAPed samples obtained by EBSD, and some detailed microstructural information is given in Table 2. In the initial material (Fig. 3a and b),

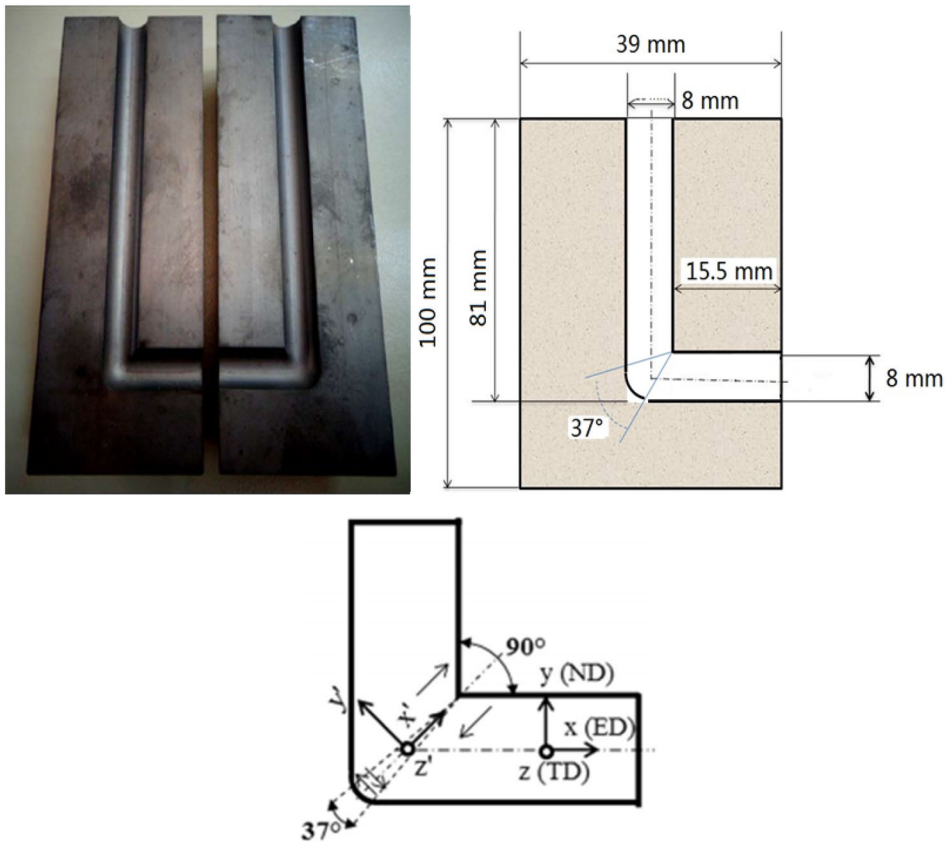

Fig. 1 Dimensions of the die used for ECAP process showing the inner angle of Φ = 90° and an outer angle of ψ = 37°. The reference system used in this study (below)

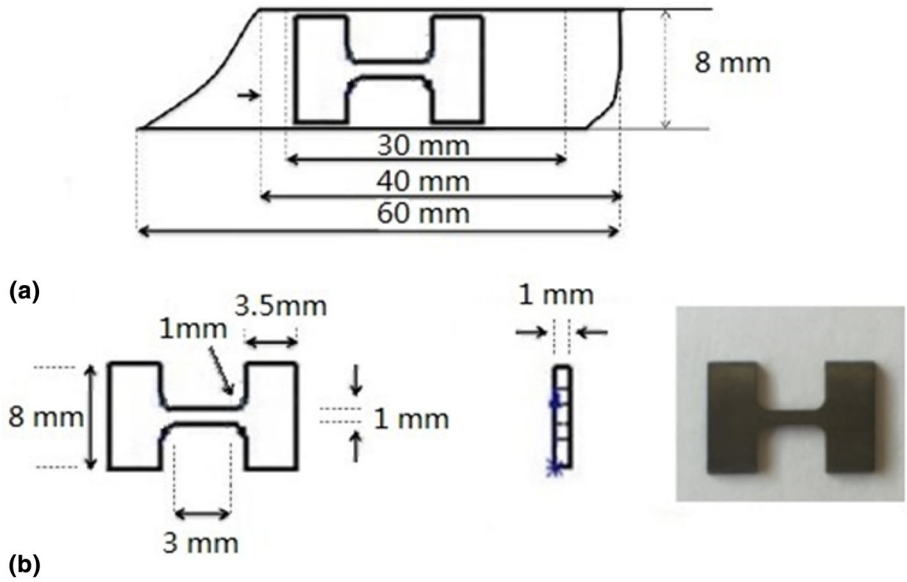

Fig. 2 (a) Extraction of the micro-tensile samples from the ECAP samples. (b) Dimensions of the micro-tensile samples used in this work

equiaxed austenite grains with some annealing twins can be observed. After one ECAP pass at room temperature (Fig. 3c and d), the grains appear extremely elongated in the shear direction, whereas the average grain size is sharply reduced. Nearly all the observed grains have developed subgrains, which is consistent with the high increase in low-angle grain boundaries (LAGB). In addition, bundles of mechanical twins are fairly easy to see. In the case of the material after one ECAP pass at 300 °C (Fig. 3e and f), the grains are also elongated in the shear direction, but there is a smaller refinement of the structure. The average grain size is clearly larger than in the case of the room temperature process. At high temperature, it is

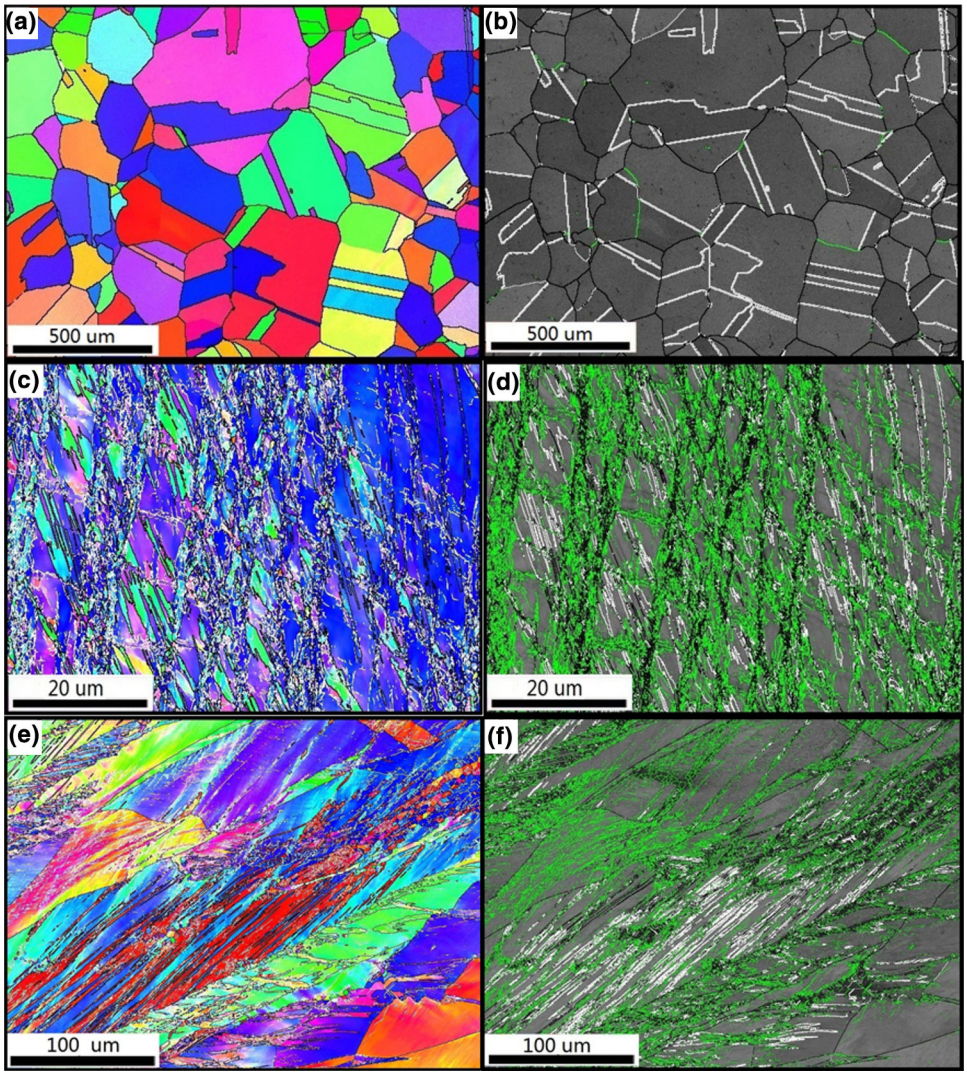

Fig. 3 EBSD IPF grain map of (a) initial sample (c) 1 pass at room temperature sample and (e) 1 pass at 300 °C sample, EBSD grain boundary map of (b) initial sample, (d) 1 pass at room temperature sample and (f) 1 pass at 300°C sample (Black line: high-angle grain boundary, green line: low-angle grain boundary, white line: twin boundary) (Color figure online)

Table 2 Microstructure characterization information of the investigated material

	Grain size (μm)			Misorientation	
ECAP condition	With twinning	Without twinning	Fraction of ∑3 grain boundary, %	HAGB (%)(including twins)	LAGB, %
0 pass	69.2	99.0	41.3	92.9	7.1
1 pass at room temperature	1.25	1.83	14.8	40.1	59.9
1 pass at 300 °C	3.9	6.9	13.4	41.3	58.7

also evident a large dislocation activity inside the deformed grains since numerous LAGB can be observed. The presence of mechanical twins is rather usual, and the twin fraction is only slightly lower than in the case of the room temperature material. This indicates that although the increase in the SFE with temperature above the range of 12-35 mJ/m^2, the TWIP steel deforms by twinning in ECAP process (Ref 18). However, the microstructure is less homogeneous than in the room temperature process and some grains appear with a lower density of subgrains and mechanical twins. The effect of temperature is also reflected in the measured values of twin thickness. In the initial material, the annealing twins have a thickness of 47.2 ± 35 μm. After ECAP at 300 °C, the twin thickness decreases to 1.03 ± 0.8 μm and in the case of ECAP at room temperature the value is only 0.4 ± 0.3 μm.

3.1.2 TEM Analysis. Figure 4 shows a bright field TEM image for the annealed sample. In the initial stage prior to deformation long dislocations can be seen, with few intersections

between them. However, the microstructure changes significantly after one ECAP pass. The TEM images corresponding to the samples after one ECAP pass at 300 °C are shown in Fig. 5. As exposed in the EBSD studies, deformation twins organized in bundles are quite obvious within the grains (as indicated by dashed lines in Fig. 5a). At higher magnifications, zones with very narrow twins can now be observed with the occasional presence of a secondary twinning system (Fig. 5b). Secondary twinning has been described in FeMnC TWIP steel processed by ECAP at 300 °C (Ref 18), but in the present case of a FeMnCAl in which a large reduction in secondary mechanical twinning has been reported (Ref 27-29), its presence must be much lower. Finally, it is interesting to note that the dislocation density inside the twins increases sharply after ECAP at warm temperature (Fig. 5c).

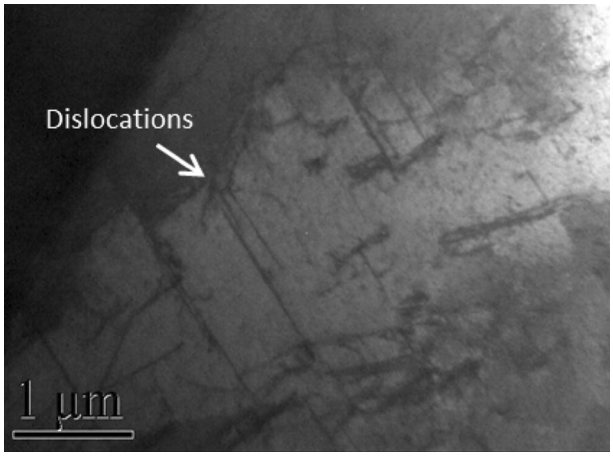

Fig. 4 TEM bright field images of the TWIP steel in the initial condition

The TEM images of the ECAPed sample at room temperature (Fig. 6) show clearly that the mechanical twins are finer than in the case of ECAP at 300 °C. At room temperature, the presence of secondary twins is more usual and more types of secondary twinning are activated. One of these types is when two twinning systems are sequentially activated (Fig. 6b). This case has been described in FeMnC TWIP steels deformed at low temperature by tensile tests (Ref 30) and by ECAP at 300 °C, although in the latter case the twins inside the primary twins were described as nano-twins (Ref 18). Another case is when two systems are simultaneously activated (Fig. 6c). This higher density of thinner twins in the samples deformed at room temperature reinforced the idea that in this material the accumulation of defects by dislocation and twin interactions is larger and the possibility to introduce more deformation is very limited.

3.2 Mechanical Behavior

The true stress-strain curves of the annealed TWIP steel and the one pass samples (both ECAPed at room temperature and at 300 °C) are shown in Fig. 7. The corresponding data are summarized in Table 3. The annealed material shows good mechanical properties, combining high ultimate tensile strength (UTS) above 1300 MPa and large ductility (total true strain close to 0.5) with a moderate yield strength (YS) of 590 MPa. The tensile curve corresponding to the sample with one ECAP pass at room temperature shows a large increase in yield

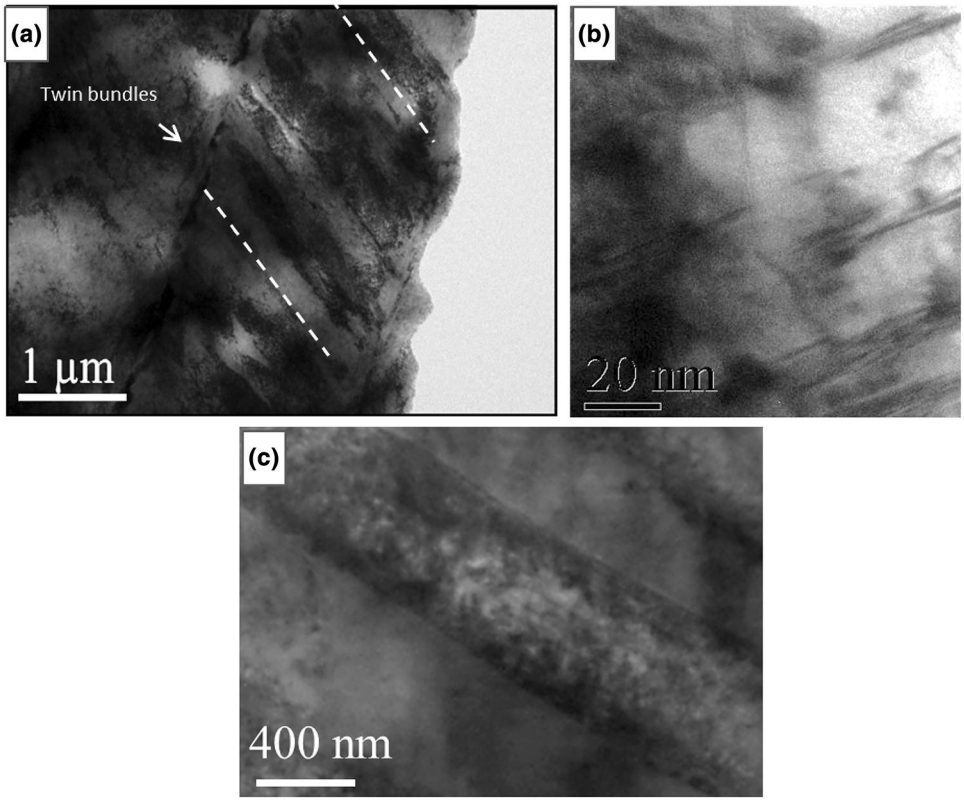

Fig. 5 TEM micrographs of material processed one pass at 300 °C: (a): general view of twins; (b): fine primary twins with traces of secondary twins; (c): high density of dislocations inside a mechanical twin

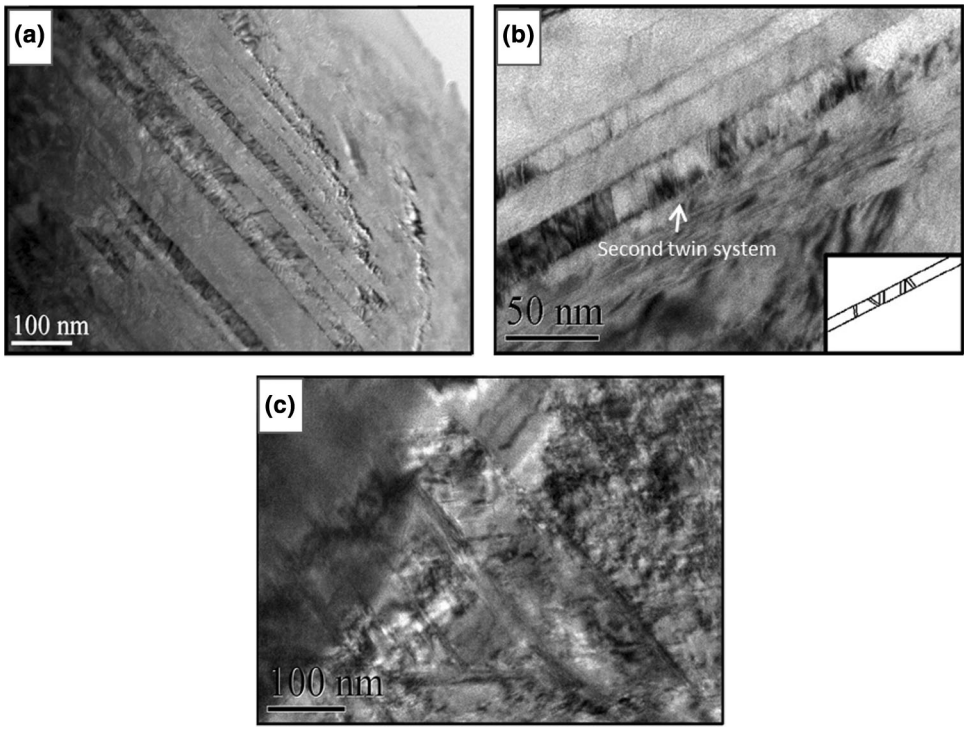

Fig. 6 TEM micrographs of the material processed one pass at room temperature: (a) general view of twins; (b) and (c) presence of secondary twinning

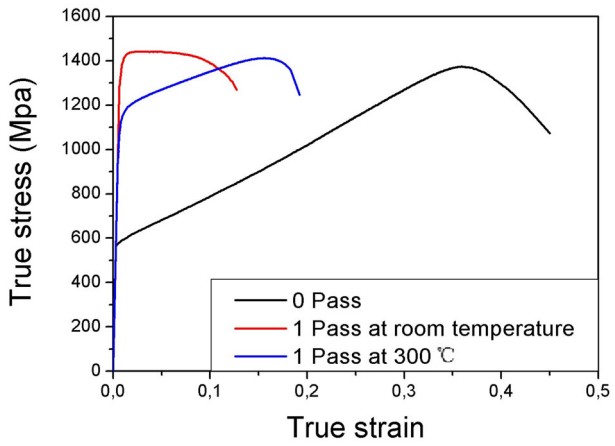

Fig. 7 Tensile true stress-strain curves of the TWIP steels in the different processing conditions

strength from the annealing state (up to 1295 MPa). The UTS reaches up to 1440 MPa, which is the maximum strength obtained, but the lowest ductility. As a consequence of this, the energy absorption capability (toughness described as a measure of the region of the plastic area of the stress-strain curve) decreases sharply. For the material with one ECAP pass at 300 °C, an intermediate behavior can be observed, whereas the increase in YS and UTS is significant (1150 and 1400 MPa, respectively) but lower than in the case of ECAP at room temperature, a relatively high total elongation of 19% is maintained.

The fracture surface for the three studied samples is shown in Fig. 8. The as-received sample displays a large ductility, and fracture occurs by void coalescence and growth. Lower amount of voids and dimples are observed in general in the ECAPed samples, where some cleavage, as well as a subcell structure (typical of fine-grained material), is apparent. According to Yanagimoto et al. (Ref 31), there are two different types of dimples for ductile fracture: the larger dimples are formed by the decohesive mechanism in the inclusion-matrix interphase, and the smaller dimples are caused by the dislocation interaction mechanism (Ref 24). After ECAP pressing, the size of the dimples is finer and more diversified (see Fig. 8b and c); there are more small dimples in the fracture surface of ECAP-ed samples than in the annealed one. The reason is that the dislocation density increases significantly and it is easier for dislocations to reach the grain boundary after one pass of ECAP, so that the transformation of the dislocations into multiple unstable crack initiation, which is the nucleus of cavity, is more convenient to take place. Although both samples deformed by ECAP have similar features, the sample after one pass at 300 °C shows higher ductility than the sample pressed at room temperature, which is in line with the tensile test results. In the samples deformed by ECAP at 300 °C, the size of its cavities is larger and the zones of cleavage and subcell structures are smaller.

A better evaluation of the ductility is the reduction in area (%RA) of the fractured specimen. This was done in the present case through scanning electron microscope due to the reduced size of the samples (Ref 32). As noticed in Table 3, the reduction in area decreases in the samples processed by ECAP, especially at room temperature. This result was expected from the tensile tests, but is important to note that the value for the samples after one ECAP pass at 300 °C is relatively high, despite the fact that the corresponding elongation value is lower. On the other hand, the sample deformed at room temperature has a low value of RA% in concordance with the more fragile aspect of the fracture surface.

Table 3 Yield strength (YS), unltimate tensile strength (UTS), YS/UTS ratio (YR), elongation toughness (area below the tensile curve) and reduction in area (%RA) of steel in different conditions

	YS, MPa	UTS, MPa	YR	Total elongation, %	Tensile toughness, J/m^3 10^3	Reduction in area, %RA
As-received	590	1370	0.45	40	489.3	64
1 ECAP PASS (300 °C)	1150	1400	0.82	19	256.5	36
1 ECAP PASS (RT)	1295	1440	0.90	13	176.16	19

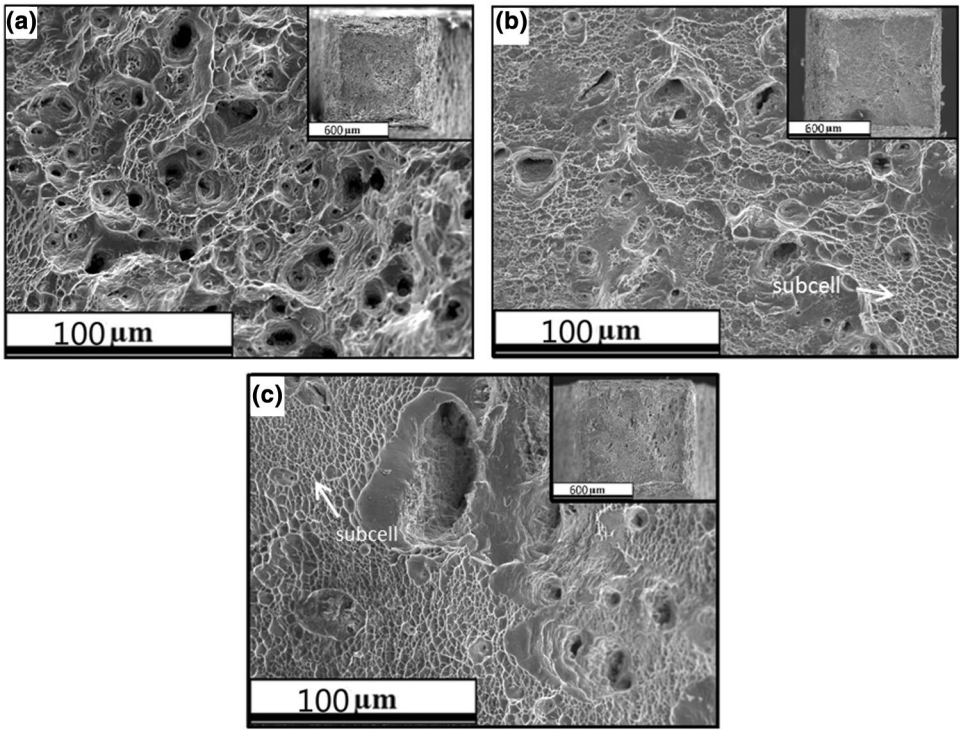

Fig. 8 Fracture surfaces of TWIP steel after tensile test (a) initial condition, (b) 1 pass at room temperature, (c) 1 pass at 300 °C

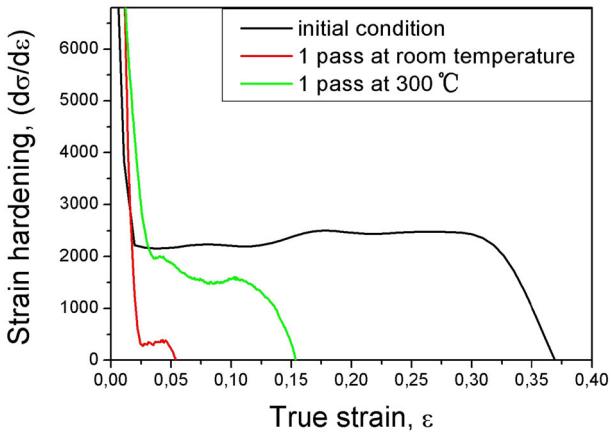

Fig. 9 Variation of the strain hardening rate with the true strain in the tensile test for the initial material and after ECAP processing

The strain hardening rate versus true strain is shown in Fig. 9 for the present TWIP steel. It can be noticed that the curve shows a pronounced drop from high strain hardening rate levels, reaching a constant level up to a strain of 0.12. After this, there is a slight increase in strain hardening rate which again remains almost constant up to 0.3 where a drop of the strain hardening rate starts until the sample ruptures at 0.37 strain. The strain hardening behavior of as-received condition sample is relatively similar to the one reported by Jin et al. (Ref 27) who investigated the mechanical properties of a Fe-18Mn-0.6C-1.5Al TWIP steel and indicated that the reduced strain hardening rate at the large strain region should be attributed to the deceleration of deformation twinning rate due to the effect of aluminum content on SFE. In the case of FeMnC TWIP steels, the SFE is maintained at lower values and the twinning activity at room temperature is larger. This is reflected in a large increase in hardening in the beginning of the plastic deformation region for the FeMnC TWIP steel (Ref 33). Therefore, for the present FeMnCAl TWIP steel it may be said that the annealed material with large grain size is able to develop during tensile test a fine twin substructure that acts as an obstacle to dislocation glide and allows a large period of strain hardening based in the dynamic Hall-Petch effect (Ref 6, 7). The material hardens until further refinement of the combined structure creates difficulties to dislocation storing which results in a decrease in strain hardening rate and final fracture (Ref 27, 33).

In the case of the material deformed by ECAP at 300 °C, a great reduction in the grain size is observed, from 69 to 3.9 μm, and the microstructure contains a large number of grains that has developed a refined structure in which appear fine mechanical twins and dislocation subgrains (Fig. 3e and f). This is reflected in the high increase in the yield strength, from 590 to 1150 MPa. In contrast to this, there are other grains that have not suffered this combined effect to such an extent. This deformed structure combined with the decrease in the grain size is reflected in the reduction in the work hardening period for the material obtained by ECAP at 300 °C comparing with the annealed one, from a strain of 0.37 to 0.15. However, in the case of the work hardening rate the decrease is less severe, and the material is able to stabilize this rate from 0.07 to 0.13. In addition, in this stage even a slight increment of the work hardening rate is observed. The existence of a period in which the work hardening rate remains constant with plastic strain in this FeMnCAl TWIP steel can be related not only to dislocation activity but also to the presence of mechanical twinning. There are two aspects that support the presence of mechanical twinning: First, the tensile tests were carried out at room temperature, which results in a low critical stress for twinning (Ref 19). Second, the presence in the microstructure of less deformed grains in which further microstructure refinement can be achieved. The observed increase in the strain hardening rate suggests that these two aspects have more importance than the expected decrease in the twin fraction as the grain size decreases, caused by a reduction in the number of nucleation sites for twins (Ref 34). The stabilization of the strain hardening rate enables the uniform elongation, and then this material shows a very high UTS of 1400 MPa.

On the other hand, the sample ECAPed at room temperature shows a quite low strain hardening capability, as it only reaches a plateau after a small strain and then falls to zero. In this case, the initial microstructure has a finer grain size than in the case of ECAP at 300 °C and within the grains a denser combination of subgrains and mechanical twins can be observed. This structure is reflected in a high yield strength of 1295 MPa. In addition, the EBSD studies have shown that this material has a slightly larger fraction of mechanical twins and the TEM studies allow to see a larger presence of secondary twinning, even with nano-twins inside the primary twins (Ref 18). Unlike ECAP at 300 °C, in which some dynamic recovery are expected during severe plastic deformation (Ref 18, 19, 35), the room temperature microstructure has less possibilities to dislocation motion and creation of subgrains that help to accommodate the deformation. Accordingly, the number and density of defects is higher and the structure has very limited ability to enable dislocation motion or to create new deformation twins, which finally results in a very limited period of strain hardening (0.05). As a result, the UTS has less increment from yield strength than in the case of the samples processed by ECAP at 300 °C, arriving to 1440 MPa.

In the three materials, the final UTS values are very similar. It could be explained thinking that independently of the type of deformation process, in all the cases the introduction of defects basically by dislocation glide and mechanical twins has reached or is very close to a saturation level. In this situation, taking into account the dynamic Hall-Petch effect described for these steels, the final strength in all cases could be similar. For the ECAP process at room temperature, there is an absence of strain hardening, and this microstructure would be the closest to saturation. In fact, this material has the higher UTS. In the ECAP process at 300 °C and in the annealed samples, although to different extent, there is the chance of deformation twinning and then strain hardening is possible. After deformation, both materials would finally arrive to the dense microstructure combination of subgrains and fine mechanical twins that produces a decrease in strain hardening. In this sense, both materials could reach similar UTS values and at the same time this UTS might be lower than in the case for ECAP at room temperature.

Comparing the present FeMnCAl TWIP steel with the FeMnC TWIP steel deformed by ECAP with passes at 300 and 400 °C (Ref 18), it must be said that the behavior is similar, with a large increase in YS and UTS together with a lower but acceptable ductility in which hardening is present. Finally, the FeMnC TWIP steel processed by ECAP at high temperatures has a larger UTS than the present FeMnCAl steel, but this can be connected with the larger twinning activity in FeMnC TWIP steel due to the absence of aluminum that increase the SFE (Ref 18, 27).

4. Conclusions

The use of an ECAP die with an inner angle of $\Phi = 90°$ and an outer angle of $\psi = 37°$ has enabled to severely deform a FeMnCAl TWIP steel by ECAP at room temperature only until 1 pass. Further deformation was not achieved due to fractures in punch and samples.

After one ECAP pass at room temperature, there is a strong reduction in the grain size from 99 to 1.8 μm together with a high increase in mechanical twins and subgrains caused by dislocation glide rendering a homogeneous and dense microstructure. Secondary twinning is very active, and twin thickness is well below 1 μm. On the contrary, the material after one pass at 300 °C shows also an important reduction in grains size but lower than the process at room temperature. There is a significant number of mechanical twins and a high density of subgrains, but the microstructure is less homogeneous than in the case of ECAP at room temperature.

The yield strength of the annealed material is increased from 590 to 1295 MPa when deformed by ECAP at room temperature, and the ultimate tensile strength arrives to 1440 MPa. The ductility is greatly reduced with no presence of strain hardening, and this might be due to the reduced grain size and the high density of subgrains that prevent the material from twinning and dislocation motion. In the case of ECAP at 300 °C, the yield strength and ultimate tensile strength rise to 1100 and 1400 MPa, and ductility reaches a 19%. In this case, the material retain some ability to harden probably related to the existence of grains in which mechanical twinning is still possible and consequently there is a period in which strain hardening is stabilized.

Acknowledgments

The present paper is financially supported by China Scholarship Council (CSC) and technically supported by the Electron Microscopy Service (EBSD analysis) in the Center Technology of Manresa (CTM) and the Transmission Electron Microscope Service (TEM analysis) in Centres Científics i Tecnològics of University of Barcelona (CCIT, UB).

References

1. X.H. Liu, W. Liu, J.B. Liu, and K.Y. Shu, Current Situation of the TWIP Steels, *Mater. Rev.*, 2010, **24**, p 102–111
2. T. Senuma, Physical Metallurgy of Modern High Strength Steel Sheets, *ISIJ Int.*, 1984, **41**, p 520–532
3. K.M. Rahman, V.A. Vorontsov, and D. Dye, The Effect of Grain Size on the Twin Initiation Stress in a TWIP Steel, *Acta Mater.*, 2015, **89**, p 247–257
4. S. Allain, J.P. Chateau, O. Bouaziz, S. Migot, and N. Guelton, Correlations Between the Calculated Stacking Fault Energy and the Plasticity Mechanisms in Fe-Mn-C Alloys, *Mater. Sci. Eng. A*, 2004, **387–389**, p 158–162
5. J.A. Jimenez and G. Frommeyer, Analysis of the Microstructure Evolution During Tensile Testing at Room Temperature of High-Manganese Austenitic Steel, *Mater. Charact.*, 2010, **61**, p 221–226
6. O. Bouaziz, S. Allain, C.P. Scott, P. Cugy, and D. Barbier, High Manganese Austenitic Twinning Induced Plasticity Steels: A Review of the Microstructure Properties Relationships, *Curr. Opin. Solid State Mater. Sci.*, 2011, **15**, p 141
7. H. Idrissi, K. Renard, L. Ryelandt, D. Schryvers, and P. Jacques, On the Mechanism of Twin Formation in Fe-Mn-C TWIP Steels, *Acta Mater.*, 2010, **58**, p 2464–2476
8. I. Mejia, A.E. Salas-Reyes, A. Bedolla-Jacuinde, J. Calvo, and J.M. Cabrera, Effect of Nb and Mo on the Hot Ductility Behavior of a High-Manganese Austenitic Fe-21Mn-1.3Al-1.5Si-0.5C TWIP Steel, *Mater. Sci. Eng. A*, 2014, **616**, p 229–239
9. A.E. Salas-Reyes, I. Mejia, A. Bedolla-Jacuinde, A. Boulaajaj, J. Calvo, and J.M. Cabrera, Hot Ductility Behavior of High-Mn Austenitic Fe-22Mn-1.5Al-1.5Si-0.45C TWIP Steels Microalloyed with Ti and V, *Mater. Sci. Eng. A*, 2014, **611**, p 77–89
10. F. Reyes-Calderon, I. Mejia, and J.M. Cabrera, Hot Deformation Activation Energy (QHW) of Austenitic Fe-22Mn-1.5Al-1.5Si-0.4C TWIP Steels Microalloyed with Nb, V, and Ti, *Mater. Sci. Eng. A*, 2013, **562**, p 46–52
11. F. Reyes-Calderon, I. Mejia, A. Boulaajaj, and J.M. Cabrera, Effect of Microalloying Elements (Nb, V and Ti) on the Hot Flow Behavior of High-Mn Austenitic Twinning Induced Plasticity (TWIP) Steel, *Mater. Sci. Eng. A*, 2013, **560**, p 552–560
12. O. Bouaziz, S. Allain, and C. Scott, Effect of Grain and Twin Boundaries on the Hardening Mechanisms of Twinning-Induced Plasticity Steels, *Scripta Mater.*, 2008, **58**, p 484–487
13. D.B. Santos, A.A. Saleh, A.A. Gazder, A. Carman, D.M. Duarte, E.A.S. Ribeiro, B.M. Gonzalez, and E.V. Pereloma, Effect of Annealing on the Microstructure and Mechanical Properties of Cold Rolled Fe-24Mn-3Al-2Si-1Ni-0.06C TWIP Steel, *Mater. Sci. Eng. A.*, 2011, **528**, p 3545–3555
14. S. Kang, Y.S. Jung, J.H. Jun, and Y.K. Lee, Effects of Recrystallization Annealing Temperature on Carbide Precipitation, Microstructure, and Mechanical Properties in Fe-18Mn-0.6C-1.5Al TWIP Steel, *Mater. Sci. Eng. A*, 2010, **527**, p 745–751
15. M.S. Matoso, R.B. Figueiredo, M. Kawasaki, D.B. Santos, and T.G. Langdon, Processing a Twinning-Induced Plasticity Steel by High-Pressure Torsion, *Scripta Mater.*, 2012, **67**, p 649–652
16. M.M. Abramova, N.A. Enikeev, J.G. Kim, R.Z. Valiev, M.V. Karavaeva, and H.S. Kim, Structural and Phase Transformation in a TWIP Steel Subjected to High Pressure Torsion, *Mater. Lett.*, 2016, **166**, p 321–324
17. E. Bagherpour, M. Reihanian, and R. Ebrahimi, On the Capability of Severe Plastic Deformation of Twining Induced Plasticity (TWIP) Steel, *Mater. Design*, 2012, **36**, p 391–395
18. I.B. Timokhina, A. Medvedev, and R. Lapovok, Severe Plastic Deformation of a TWIP Steel, *Mater. Sci. Eng. A*, 2014, **593**, p 163–169
19. C. Haase, O. Kremer, W. Hu, T. Ingendahl, R. Lapovok, and D. Modolov, Equal-Channel Angular Pressing and Annealing of a Twinning-Induced Plasticity Steel: Microstructure, Texture and Mechanical Properties, *Acta Mater.*, 2016, **107**, p 239–253
20. L. Remy, Kinetics of f.c.c. Deformation Twinning and Its Relationship to Stress-Strain Behaviour, *Acta Metall.*, 1978, **26**(3), p 443–451
21. Y. Dastur and W. Leslie, Mechanism of Work Hardening in Hadfield Manganese Steel, *Metall. Trans. A*, 1981, **12**(5), p 749–759
22. J.-L. Collet, F. Bley, A. Deschamps, and C. Scott, Study of the Deformation Mechanisms of TWIP Steels (Fe-Mn-C) by x-ray Diffraction, *Adv. Mater. Res.*, 2007, **15–17**, p 822–827
23. Y. Iwahashi, Z. Horita, M. Nemoto, and T.G. Langdon, An Investigation of Microstructural Evolution During Equal-Channel Angular Pressing, *Acta Mater.*, 1997, **45**, p 4733–4741
24. O.F. Higuera-Cobos and J.M. Cabrera, Mechanical, Microstructural and Electrical Evolution of Commercially Pure Copper Processed by Equal Channel Angular Extrusion, *Mater. Sci. Eng. A*, 2013, **571**, p 103–114
25. L. Lin and T.Y. Hsu, Gibbs Free Energy Evaluation of the FCC and HCP Phases in Fe-Mn-Si Alloys, *Calphad*, 1997, **21**, p 443–448
26. A. Dumay, J.P. Chateau, S. Allain, S. Migot, and O. Bouaziz, Influence of Addition Elements on the Stacking-Fault Energy and Mechanical Properties of an Austenitic Fe-Mn-C Steel, *Mater. Sci. Eng. A*, 2008, **483–484**, p 184–187
27. J.-E. Jin and Y.-K. Lee, Strain Hardening Behavior of a Fe-18Mn-0.6C-1.5Al TWIP Steel, *Mater. Sci. Eng. A*, 2009, **527**, p 157–161
28. Y.T. Zhu, X.Z. Liao, and X.L. Wu, Deformation Twinning in Nanocrystalline Materials, *Prog. Mater. Sci.*, 2012, **57**, p 1–62
29. C.X. Huang, Y.L. Gao, and G. Yang, Bulk Nanocrystalline Stainless Steel Fabricated by Equal Channel Angular Pressing, *J. Mater. Res.*, 2006, **21**(7), p 1687–1692
30. D. Barbier, N. Gey, S. Allain, N. Bozzolo, and M. Humber, Analysis of the Tensile Behavior of a TWIP Steel Based on the Texture and Microstructure Evolutions, *Mater. Sci. Eng. A*, 2009, **500**, p 196–206
31. J. Yanagimoto, J. Tokutomi, K. Hanazaki, and N. Tsuji, Continuous Bending-Drawing Process to Manufacture the Ultrafine Copper Wire with Excellent Electrical and Mechanical Properties, *CIRP Ann. Manuf. Technol.*, 2011, **60**, p 279–282
32. M. Besterci, T. Kvackaj, L. Kovac, K. Sulleiova, and P. Kulu, Mechanical Properties and Fracture of Nanocopper by Severe Plastic Deformation, *Proc. Estonian Acad. Sci. Eng.*, 2006, **12**, p 340–348
33. I. Gutierrez-Urrutia and D. Raabe, Dislocation and Twin Substructure Evolution During Strain Hardening of an Fe-22 wt.% Mn-0.6 wt.%. C TWIP Steel Observed by Electron Channeling Contrast Imaging, *Acta Mater.*, 2011, **59**, p 6449–6462
34. I. Gutierrez-Urrutia and D. Raabe, Grain Size Effect on Strain Hardening in Twinning-Induced Plasticity Steels, *Scripta Mater.*, 2012, **66**, p 992–996
35. C.X. Huang, G. Yang, Y.L. Gao, S.D. Wu, and Z.F. Zhang, Influence of Processing Temperature on the Microstructures and Tensile Properties of 304L Stainless Steel by ECAP, *Mater. Sci. Eng. A*, 2008, **485**, p 643–650